ACS Catalysis

pubs.acs.org/acscatalysis Research Article

DiploPhos: A Hemilabile Bisphosphine for Sterically Hindered Ni-Catalyzed Suzuki–Miyaura Couplings

T. Judah Raab,§ Hang Chi Ho,§ Tyler Kerr, Nari Tao, Shashank Shekhar, Rafal Swiatowiec, Michael C. Haibach,* and Abigail G. Doyle*

Cite This: https://doi.org/10.1021/acscatal.6c05422 Read Online

ACCESS | Metrics & More | Article Recommendations | Supporting Information

ABSTRACT: Pharmaceutically relevant Suzuki–Miyaura cross-couplings (SMCs) often require designer phosphine ligands and palladium loadings above 1 mol % to couple Lewis basic, sterically congested substrates. Recent work has demonstrated that nickel is an attractive alternative to palladium for facile SMCs, but further ligand development is required for Ni catalysis to rival Pd for more challenging couplings. We applied prior work on monophosphine ligand design for Ni to develop a bisphosphine, DiploPhos, that outperforms state-of-the-art ligands for Ni to achieve sterically hindered Ni SMCs with ≥3 *ortho*-substituents. Catalyst speciation studies revealed the hemilabile nature of DiploPhos, which improves reactivity relative to stronger chelating ligands but also leads to the formation of less-active DiploPhos-bridged aggregates. Lewis basic functionality (present on substrates or additives) was found to promote the disaggregation of these species and led to increased SMC yields. This observation is contrary to most other systems in which Lewis basic substrates inhibit Ni-catalyzed SMC reactions. Ligand exchange studies demonstrated that despite its hemilability, DiploPhos is more resistant to displacement by heterocycles than similar bisphosphines. Together, these properties led to best-in-class reactivity for sterically hindered, Lewis base-rich Ni SMCs.

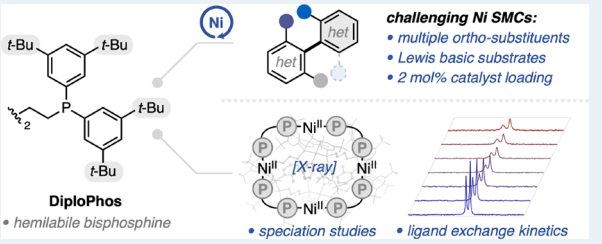

KEYWORDS: *Ni catalysis, Suzuki–Miyaura, phosphines, ligand design, cross-coupling, organometallic studies*

1. INTRODUCTION

Transition metal-catalyzed cross-coupling reactions are an indispensable part of the synthetic chemistry toolkit. One of the most ubiquitous reactions in this class is the Suzuki–Miyaura cross-coupling (SMC), which couples aryl electrophiles and arylboron species to form $C(sp^2)$–$C(sp^2)$ bonds, typically with palladium catalysts. Extensive research led to the development of specially tailored phosphine ligands for Pd-catalyzed SMCs,[1,2] enabling more efficient catalysis and broader compatibility with complex substrates. These advances have had a profound impact on the discovery and manufacturing of pharmaceutical compounds.[3,4]

Environmental and economic considerations have motivated the exploration of alternatives to Pd catalysis for SMC reactions. Nickel, palladium's more earth-abundant base metal congener, has emerged as a promising alternative to Pd, with recent examples of Ni-catalyzed SMCs demonstrating promising efficiency and scalability.[5−11] While some examples demonstrate that Ni SMCs can proceed even in the absence of ancillary ligands, advances in ligand design are necessary to address several synthetic limitations.[8−10,12] Specifically, few known Ni-catalyzed SMCs engage sterically hindered, Lewis basic substrate classes. Such coupling reactions can be used to construct biaryl motifs in pharmaceuticals (e.g., the $KRAS^{G12C}$ inhibitor Sotorasib) and ligand or catalyst derivatives (Figure 1A).[13,14] While Pd catalysts have been reported to mediate this class of coupling reaction, Ni catalysts that can form such hindered bonds are virtually unknown—only one literature Ni SMC affords tri-*ortho*-substituted products, and this method is demonstrated solely on binaphthyl compounds.[15] The differences between Pd and Ni catalysts can be attributed to the extensive ligand design done for Pd, which has not directly translated to Ni-catalyzed SMCs. Typically, Pd-catalyzed SMCs are promoted by sterically bulky monophosphine ligands that favor monoligated Pd species (P_1Pd), but many such ligands fail for Ni—likely due to differences in the metals' size (Figure 1B).[16,17]

Recent mechanistic studies that probe these reactivity differences have indicated that bisligated Ni species (P_2Ni) must be favored to avoid off-cycle reactivity,[17] but access to monoligated intermediates can lead to rate acceleration of key steps in the catalytic cycle (Figure 1C).[18] As such, ligand design for Ni-catalyzed SMCs has focused on moderately sized monophosphine ligands

Received: July 13, 2026
Revised: August 10, 2026
Accepted: August 11, 2026

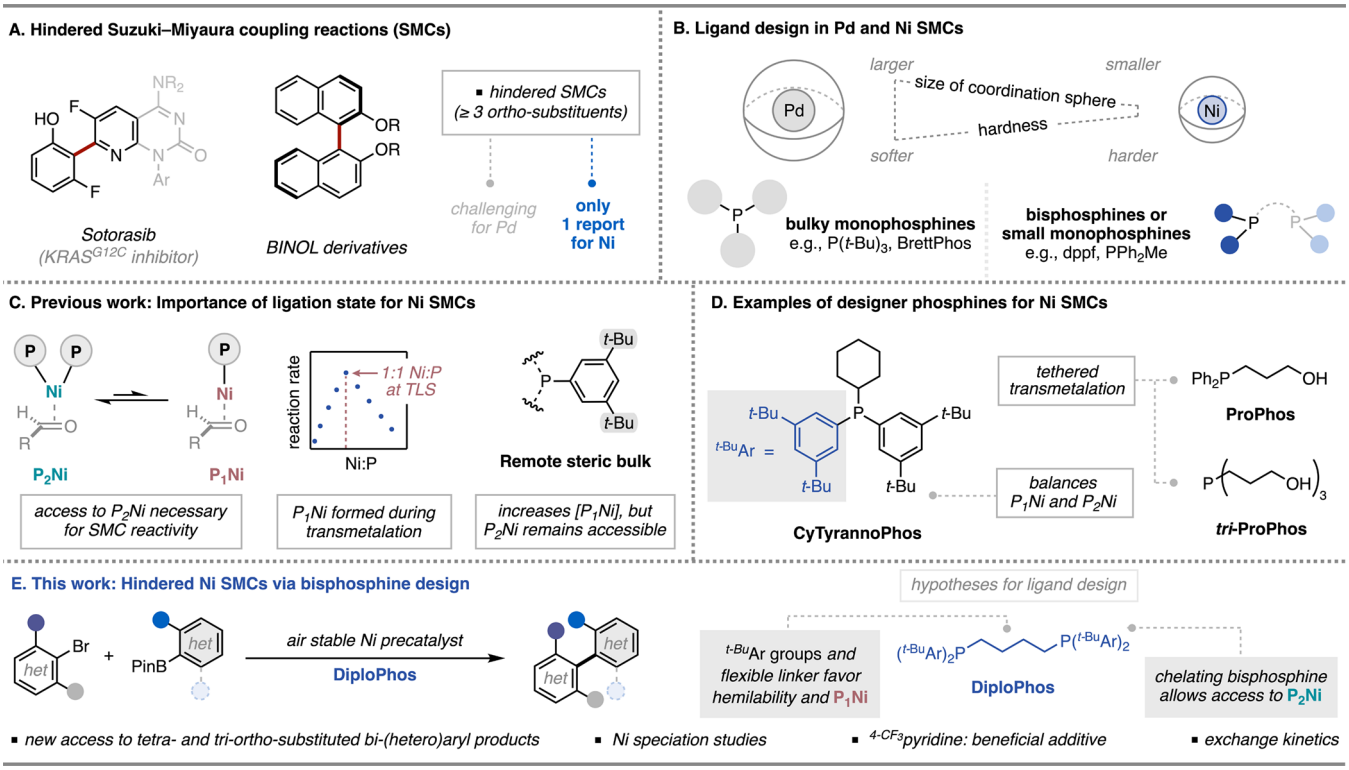

Figure 1. (A) Application of sterically hindered SMC reactions and literature precedent. (B) Metal properties and ligand design principles relevant to Pd- and Ni-catalyzed SMC reactions. (C) The role of ligation state in Ni-catalyzed SMC reactions. (D) Examples of phosphine ligands designed for Ni-catalyzed SMCs. (E) This work.

(Figure 1D). For example, the Doyle group's DinoPhos ligands—which are characterized by sterically bulky groups distal to phosphorus—are observed to form P_2Ni species. However, for the DinoPhos ligand CyTyrannoPhos (cyclohexylbis(3,5-di-*tert*-butylphenyl)phosphine), the active species in transmetalation has been shown to be monoligated (Figure 1C), and the ligand's remote steric bulk has been proposed to promote the formation of P_1Ni intermediates relative to CyTyrannoPhos's undecorated analogue $CyPPh_2$.[18] Similarly, the Diao group's ProPhos and *tri*-ProPhos—monophosphines which accelerate transmetalation by tethering the organoboron partner via pendant hydroxyl groups—have been observed to form P_2Ni species at both Ni(II) and Ni(0) (Figure 1D).[6,7]

While the majority of recent ligand design efforts for Ni-catalyzed SMCs have employed monophosphines, bisphosphines like dppb,[5] dppf,[18,19] and DPEPhos,[20,21] are also known to be effective ligands. Since bisphosphines chelate, they impart catalyst stability and satisfy the requirement for P_2Ni formation. Nevertheless, limited effort has been directed at designing bisphosphine ligands for Ni SMCs. Moreover, little is known about the speciation of Ni complexes bearing long-linker (≥4 carbons) bisphosphines, which have been proposed to form aggregates.[5]

Here, we report the use of DiploPhos, a long-linker bisphosphine ligand bearing DinoPhos-type remote steric bulk, that promotes SMCs with sterically hindered substrates that are unprecedented for Ni catalysis (Figure 1E).[22] Specifically, DiploPhos affords tri-*ortho*-substituted products containing *N*-heterocycles and tetra-*ortho*-substituted products. Even with Pd, couplings that involve such hindered bond formations are challenging, often requiring catalyst loadings ≥ 1 mol %, designer ligands, or both.[23−26] To understand the origin of the improved performance, speciation studies were conducted on DiploPhos-bound Ni complexes. Consistent with prior findings on ligation state requirements for Ni SMCs, it was found that DiploPhos is hemilabile and readily forms both P_2Ni and P_1Ni species. This hemilability led to the formation of DiploPhos-bridged aggregates, but Lewis basic substrates or additives were found to induce disaggregation, boosting SMC yields. Furthermore, VT-NMR and UV–vis experiments demonstrated DiploPhos's resistance to dissociating its second arm, consistent with the reaction's exceptional tolerance to Lewis basic heterocycles.

2. RESULTS AND DISCUSSION

2.1. Phosphine Development

In order to understand the capabilities of existing ligand frameworks and inform ligand design for challenging Ni-catalyzed SMCs, we conducted high-throughput experimentation (HTE) on three representative reactions (see Supporting Information Section S2.1). The selected reactions contained Lewis basic functionality and at least two *ortho*-substituents. Furthermore, we chose to perform these reactions with less-reactive pinacolboron esters due to their favorable stability and speciation relative to boronic acids.[27−29]

While we are unaware of literature precedent for a tetra *ortho*-substituted Ni SMC, we found that the coupling to afford 4-(2,6-dimethoxyphenyl)–3,5-dimethylpyridine could be promoted in modest yield by some mono- and bis-phosphines

https://doi.org/10.1021/acscatal.6c05422
ACS Catal. XXXX, XXX, XXX−XXX

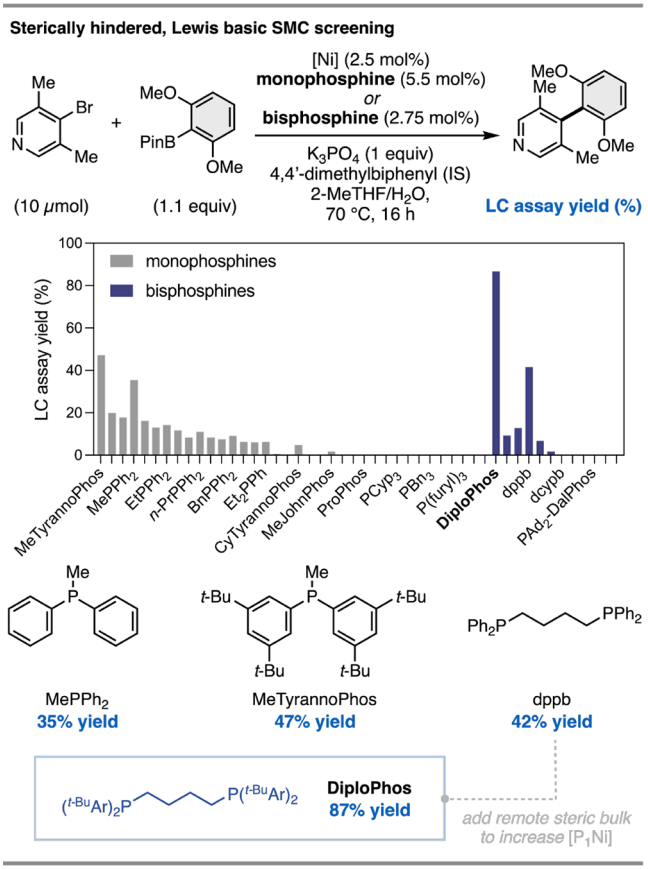

Figure 2. Top: the tetra-*ortho*-substituted model SMC reaction and HTE yields for select monophosphines (gray bars) and bisphosphines (purple bars). Bottom: three top-performing phosphine ligands and development of DiploPhos. [Ni] = (TMEDA)Ni(*o*-Tol)Cl. LC assay yields were calculated using 4,4′-dimethylbiphenyl as an internal standard.

(Figure 2, top). $MePPh_2$ was among the top performers for the reaction, consistent with its small steric profile and a prior report demonstrating its utility as a ligand for heteroaryl Ni SMCs.[30] Notably, MeTyrannoPhos (methylbis(3,5-di-*tert*-butylphenyl)phosphine), an analog of $MePPh_2$ with DinoPhos-type remote steric bulk, showed improved performance relative to $MePPh_2$ (47% and 35% yield, respectively). We hypothesized that the improved performance of MeTyrannoPhos relative to $MePPh_2$ could be attributed to its greater propensity for dissociation to give P_1Ni species, which are proposed intermediates in catalysis.[18,31] For a sterically hindered substrate pairing, this property might be expected to be particularly important to compete with off-cycle pathways. Similarly, the highest-yielding bisphosphine ligand for the reaction was dppb (di(1,4-bis(diphenylphosphino)butane), for which the flexible linker can promote formation of P_1Ni via dissociation of one phosphine arm (i.e., κ^1 binding).[5,18]

We hypothesized that the combination of DinoPhos-type remote steric bulk and a butyl linker could cooperatively promote P_1Ni formation while keeping P_2Ni accessible (Figure 2, bottom). We therefore targeted a dppb analog with 3,5-di-*tert*-butylphenyl ($^{t\text{-Bu}}$Ar) groups. The resulting ligand, DiploPhos (1,4-bis(bis(3,5-di-*tert*-butylphenyl)phosphino)butane), performed excellently in the reaction, affording the tetra-*ortho*-substituted product of the model reaction in 87% yield. While DiploPhos has not previously been used for cross-coupling chemistry, it has been studied for Ru-catalyzed hydrogenations.[32] DiploPhos is bench-stable (see Supporting Information Section 4) and has become commercially available over the course of our study.

2.2. Evaluation of Substrate Scope

To efficiently evaluate a variety of conditions for the new Ni/DiploPhos system, we conducted an optimization campaign guided by Experimental Design via Bayesian Optimization (EDBO, Supporting Information Section 2.2).[33,34] We chose to use the air-stable Ni source (TMEDA)Ni(*o*-Tol)Cl for optimization.[35,36] We found that optimal yields were obtained with a 2:1 DiploPhos/Ni ratio (see Supporting Information Section S2.3 for further evaluation of conditions), diverging from reported conditions for dppb in which a 1:1 ratio of dppb/Ni was optimal.[5] We were excited to observe that the reaction proceeded most efficiently in a process-friendly 2:1 2-MeTHF/H_2O solvent system, in which the optimal base (K_3PO_4) was fully solubilized. While K_3PO_4 was found to be the optimal base for reactivity, we also observed promising reactivity with the organic base DABCO. With these conditions, we sought to assess the substrate scope and functional group tolerance of Ni-catalyzed SMCs with DiploPhos (Figure 3). To do so, we selected substrates with a range of *ortho*-substituents and Lewis basic functionalities. For di-*ortho*-substituted SMCs, a range of *ortho*-substituents such as methyl (**1a**), trifluoromethyl (**1b**), isopropyl (**1c**) and 4-*N*-Boc-piperidinyl (**1d**) groups gave good yields ranging from 72 to 88%. Reducing the Ni loading to 1 mol % only decreased the yield of **1a** slightly, but further reduction in precatalyst loading resulted in a precipitous decrease in yield (see Supporting Information Section S2.3).

A more hindered boronic ester partner (**1e**) with 2,6-dimethyl substitution showed only 24% yield with 4-bromoacetophenone, while an SMC where both partners possess Lewis basic heteroaryl fragments (**1f**) gave good yield (83%). A range of methoxy-substituted pyridines (**1g** and **1h**) performed well, as did *N*-methyl indole (**1i**), although this coupling required an increased loading of the organoboron partner due to its propensity for protodeboronation.

We were also pleased to find that a range of biaryls bearing 3 *ortho*-substituents were accessible. Hindered aryl bromides such as 5-bromo-6-methylquinoline, 2-bromo-1,3-dimethylbenzene, as well as 1-bromo-2-isopropylbenzene (to afford **1j**, **1k**, and **1l**, respectively) gave good to moderate yields. Other heterocycles that are tolerated include an *N*-methylpyrazole (**1m**), as well as a tetrahydropyran-protected indazole (**1n**). There is scarce literature precedent for tri-*ortho*-substituted Ni SMCs, with many state-of-the-art Ni SMC methods reporting only up to di-*ortho*-substituted products.[5−7,19] To the best of our knowledge, Hong and coworkers' Sadphos ligand is the only other phosphine reported to mediate tri-*ortho*-substituted Ni SMCs, and their substrate scope contains no *N*-heterocycles and exclusively binaphthyl scaffolds.[15] Thus, the *N*-heterocyclic tri-*ortho*-substituted examples **1j**, **1k**, **1m**, and **1n** are the first of their kind furnished by a Ni SMC.

Biaryls with 4 *ortho*-substituents such as **1o** and **1p** were formed in 11 and 86% yield respectively. We hypothesize that the difference in yields between the pyrimidinyl (**1o**) and pyridyl (**1p**) aryl bromides is due to the greater electronic activation of the carbon−bromine bond in **1p**. Additionally, we found that

https://doi.org/10.1021/acscatal.6c05422
ACS Catal. XXXX, XXX, XXX−XXX

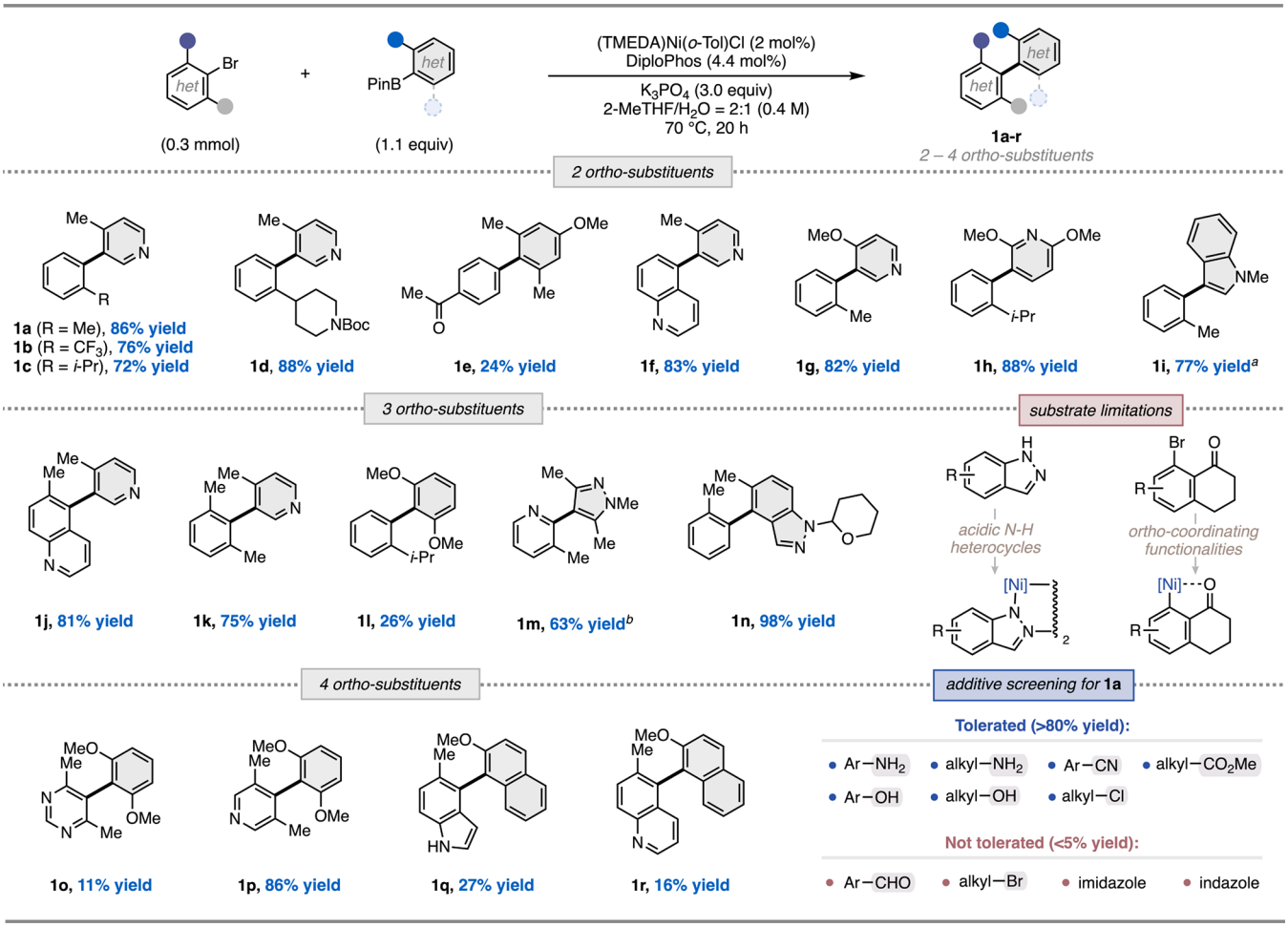

Figure 3. Substrate scope, reaction limitations, and reaction tolerance to additives. Unless otherwise indicated, yields are isolated yields on 0.3 mmol scale. [a]2.5 equivalents of boronic ester used. [b]1.0 mmol scale.

a substrate containing an unprotected indole (**1q**) proceeded with moderate yield, while a coupling to form a binaphthyl-type scaffold afforded 16% of product **1r**. While most of these tetra-*ortho*-substituted couplings give low yields, they proceed with promising turnover numbers—even with Pd, this class of SMCs require bespoke ligands, elevated temperature, and high catalyst loadings.[1,24–26,37,38]

A noteworthy limitation to these reaction conditions includes heterocycles that contain acidic N–H bonds such as unprotected imidazoles, indazoles, and benzotriazoles (Figure 3; for a full list of unsuccessful couplings, see Supporting Information Section S7.2). We hypothesize that substrates containing these heterocycles lead to the formation of inactive bimetallic species as reported for Pd-catalyzed SMCs.[38] We also found that strongly coordinating functional groups in the *ortho*-position such as ketones, amines and aryl ethers were not tolerated. One interesting feature we observed was that substrates that contain no Lewis basic functionalities (**1e** and **1l**) only performed moderately compared to couplings that possess pyridine-like nitrogen atoms, which diverges from proposals that Ni catalysts are poisoned by heterocyclic substrates in SMC reactions (see Section 2.3).[19,30]

To further evaluate the functional group tolerance of the reaction, we conducted an additive screen on the coupling to afford **1a** (see Supporting Information Section S6).[39] We observed that the Ni/DiploPhos system was able to tolerate a range of common functionalities, including protic groups such as amines, anilines, alcohols and phenols. Potentially coordinating nitrile and ester additives also did not decrease the reaction yield and could be recovered fully. Alkyl chlorides, which serve as substrates in other Ni-catalyzed cross-coupling reactions, were also tolerated, demonstrating the possibility of downstream functionalization of this functional group with other cross-coupling methodologies.[40] Meanwhile, aldehydes, which have been shown to coordinate to low-valent nickel centers,[17,41] and alkyl bromides, which can undergo halogen-atom abstraction with Ni(0) species,[42] were not tolerated in the reaction.

We also performed direct comparisons with reported ligands for Ni SMCs to evaluate whether DiploPhos was optimal for different substrate pairings (Figure 4A). We found that across scope entries, **1f**, **1j**, and **1l**, DiploPhos performed favorably relative to dppb and ProPhos.[5,6] Moreover, monophosphine analogues with other pendant functionality were found to approach the performance of DiploPhos for the coupling to afford **1j** (see Supporting Information Section S8.3), indicating that further ligand design in this area has promise. Further investigation of DiploPhos analogues for improved reactivity in challenging Ni SMCs is ongoing in our laboratories.

https://doi.org/10.1021/acscatal.6c05422
ACS Catal. XXXX, XXX, XXX–XXX

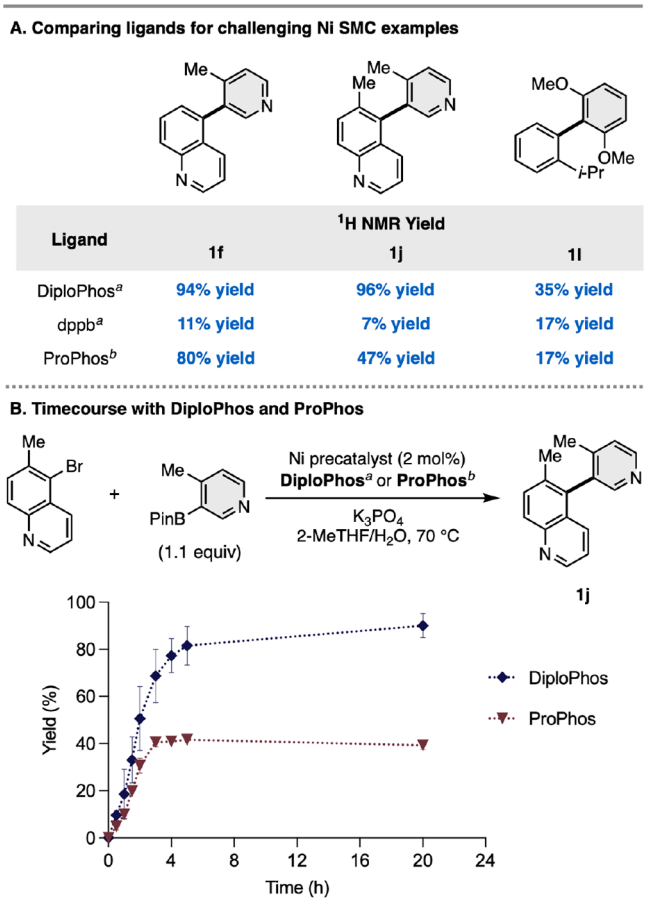

Figure 4. (A) Yield comparisons for scope examples **1f**, **1j**, and **1l** with DiloPhos, dppb, and ProPhos. Yields determined by ^{1}H NMR using 1,3,5-trimethoxybenzene as internal standard. [a]Conditions: (TMEDA)Ni(*o*-Tol)Cl (2 mol %), DiloPhos or dppb (4.4 mol %), K_3PO_4 (3.0 equiv), 2-MeTHF/H_2O = 2:1, 70 °C, 20 h. [b]Conditions: $Ni(COD)_2$ (2 mol %), ProPhos (8 mol %), K_3PO_4 (2.5 equiv), 2-MeTHF/H_2O = 5:1, 70 °C, 20 h. (B) Timecourse data for the SMC to give **1j** with DiloPhos and ProPhos. Timecourses were run in duplicate. Conditions are the same for each ligand as in panel A. Yields were determined by GC-FID using 2-fluorobiphenyl as an internal standard. Error bars are one standard deviation of two trials.

For the coupling to afford **1j**, we also gathered timecourse data for the reaction with DiloPhos and ProPhos, a state-of-the-art-ligand for Ni SMCs (Figure 4B).[6] Notably, the reaction's profile suggests that DiloPhos both accelerates turnover (faster initial rate) and prevents catalyst decomposition (more sustained product formation) relative to ProPhos.

2.3. Speciation and Reactivity Studies

The impact of remote steric bulk on ligation state has previously been studied for monophosphines.[18] However, for bisphosphines, the interplay between P_1Ni and P_2Ni species, as well as the effect of ligand structure on catalyst speciation, have not been studied in detail. Therefore, we sought to conduct studies on the role of DiloPhos's 3,5-*t*-Bu substituents, and the origins of improved reactivity.

We began by examining the structure and speciation of DiloPhos-bound Ni(0) complexes. By mixing $Ni(COD)_2$ (COD, 1,5-cyclooctadiene) and 1.0 equivalent of DiloPhos, we obtained (DiloPhos)Ni(COD) (**2**, Figure 5A). Vapor diffusion of acetonitrile into a toluene solution of **2** yielded crystals suitable for SC-XRD, allowing for comparisons to the reported structure of (dppb)Ni(COD) (**3**) and other (bisphosphine)Ni(COD) complexes (see Supporting Information Section S10.4).[43] We found that the percent buried volume at 3.5 Å ($\%V_{bur\ 3.5\ Å}$) was similar between the two complexes (54.0 and 53.3% for **2** and **3**, respectively). However, when we extended the sphere to 5.0 Å ($\%V_{bur\ 5.0\ Å}$), the remote steric bulk of DiloPhos is evident (54.5%) relative to dppb-bound **3** (49.4%). The exact cone angle, calculated using MORFEUS,[44] was found to be larger in **2** (256.1°) than in **3** (230.8°). The bite angles of the bisphosphines were found to be similar (101.5° in **2** and 101.8° in **3**). The average C=C bond lengths of COD in each complex were within error (1.391(2) Å and 1.387(4) Å for **2** and **3**, respectively), which indicates a similar degree of π-backbonding from the Ni(0) center to the COD ligand. Evidently, inclusion of the *t*-Bu groups does not markedly increase the donating ability of DiloPhos relative to dppb. Therefore, we chose to focus on the steric factors behind the improved reaction performance of DiloPhos.

To investigate speciation at Ni(0), we studied the distribution of two Ni(0) species: (bisphosphine)Ni(COD) and $(bisphosphine)_2Ni$ (Figure 5B). Complexes of the type $(bisphosphine)_2Ni$ are known to be a thermodynamic sink in catalysis for ligands such as XantPhos and dppe.[43,45,46] At 1:1 $Ni(COD)_2$:dppb, 5% of the nickel species formed was $(dppb)_2Ni$, while no $(DiloPhos)_2Ni$ was observed in the analogous experiment with DiloPhos. Increasing the loading of dppb to 2 equivalents resulted in a distribution of 67% $(dppb)_2Ni$ and 33% of **3**. Conversely, at 2:1 stoichiometry with DiloPhos, $(DiloPhos)_2Ni$ was not observed at all, with **2** being the only nickel-containing species observed by $^{31}P\{^{1}H\}$ NMR. This observation demonstrates the resistance of DiloPhos towards forming the catalyst sink $(bisphosphine)_2Ni$, which we attribute to the destabilization of $(bisphosphine)_2Ni$ by the bulky *t*-Bu groups.

With an improved understanding of the coordination chemistry of DiloPhos at Ni(0), we sought to examine its oxidative addition reactivity in a catalytic context (Figure 5C). We devised a different excess study on the coupling of an aryl bromide with two *ortho*-methyl substituents (to afford product **1k**) to determine whether oxidative addition was turnover limiting with a sterically hindered electrophile. Upon varying the initial concentration of aryl bromide ($[ArBr]_0$), no rate dependence on $[ArBr]_0$ was observed, indicating that [ArBr] is not present in the rate law for the catalytic reaction. Furthermore, ^{31}P NMR analysis of this reaction suggested that a μ-hydroxo Ni species is the resting state of the Ni catalyst (see Supporting Information Section S9.2.2). Similar species have been invoked as off-cycle catalyst resting states in Ni SMCs.[31]

Having ruled out oxidative addition as the turnover-limiting step, we turned our attention to transmetalation and the Ni(II) oxidative addition complexes (OACs) that precede this step. Such complexes are well-established to be isolable intermediates in Ni-catalyzed SMCs.[47] To this end, we conducted a ligand displacement of (TMEDA)Ni(*o*-Tol)Cl with DiloPhos (see Supporting Information Section S5).[6] The resultant orange solid possessed only one resonance in $^{31}P\{^{1}H\}$ NMR, consistent with a *trans*-bound configuration of the phosphorus nuclei. To our surprise, upon obtaining X-ray

https://doi.org/10.1021/acscatal.6c05422
ACS Catal. XXXX, XXX, XXX–XXX

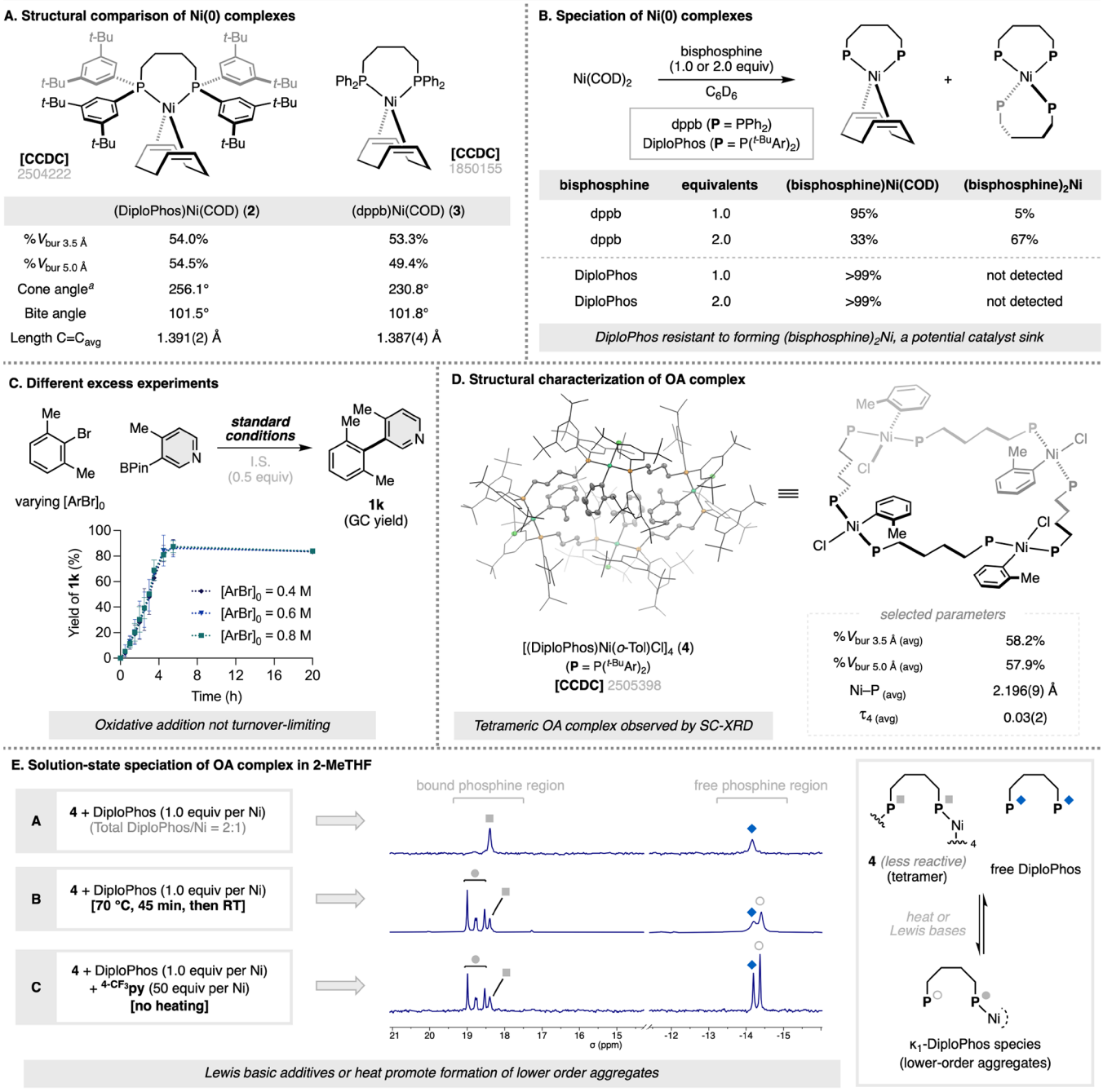

Figure 5. (A) Structural comparisons of DiploPhos and dppb-bound Ni(0) complexes **2** and **3**. [a]Cone angle calculated using MORFEUS. (B) $^{31}P\{^{1}H\}$ NMR study tracking the speciation of Ni^0 complexes with DiploPhos and dppb in C_6D_6. (C) Different excess experiments for a DiploPhos/Ni SMC with a sterically hindered aryl bromide substrate. Timecourses were run in duplicate. Yields were determined by GC-FID using 2-fluorobiphenyl as an internal standard (I.S.). Error bars are one standard deviation of two trials. (D) Solid state structure of **4**, with thermal ellipsoids displayed at 10% probability, $^{t\text{-Bu}}$Ar groups displayed as wireframes, and hydrogen atoms omitted for clarity. Ni–P distances and τ_4 parameters reported as the average of two crystallographically unique Ni centers. (E) $^{31}P\{^{1}H\}$ NMR studies demonstrating the hemilability of DiploPhos in **4**. $^{4\text{-CF}_3}$**py** = 4-trifluoromethylpyridine. For structures **2**, **3**, and **4**, buried volumes were calculated from crystal structure geometries after removing all atoms that were not part of the bisphosphine ligands and represent the size of two phosphorous centers around Ni. For more details, see Supporting Information Section S10.

quality crystals of the OAC, the complex had aggregated as tetrameric $[(DiploPhos)Ni(o\text{-Tol})Cl]_4$ (**4**, Figure 5D). Complex **4** features a macrocycle consisting of 4 Ni atoms and 4 DiploPhos molecules, with each DiploPhos molecule bridging 2 Ni centers. While $(L)_nNi(o\text{-Tol})Cl$ complexes are known for many monophosphines and bisphosphines,[47−49] none of these complexes are tetrameric in the solid state. Moreover, to our knowledge, complex **4** is the first reported crystal structure of a Ni(II) aryl halide complex bearing a bisphosphine with a flexible ≥4 carbon alkyl linker.[50,51] The tendency of DiploPhos to form

https://doi.org/10.1021/acscatal.6c05422
ACS Catal. XXXX, XXX, XXX−XXX

bridged, oligomeric species like **4** is consistent with our hypothesis that DiploPhos's remote steric bulk and flexible butyl linker promote reversible dissociation of one ligand arm.[5,18]

Having determined the solid-state structure of **4**, we further evaluated its solution-state speciation with $^{31}P\{^{1}H\}$ NMR in 2-MeTHF, the solvent used in the catalytic reaction (Figure 5E). No spectral changes were observed when mixing **4** and 1.0 equivalent per Ni of DiploPhos at ambient temperature (spectrum **A**, total DiploPhos/Ni ratio of 2:1). Heating of this mixture gave several new peaks in the bound phosphine region (solid gray circle, spectrum **B**), consistent with the conversion of tetrameric **4** to a mixture of lower order aggregates. The new peak that appears in the free phosphine region (hollow gray circle, spectrum **B**) suggests formation of species where only one arm of DiploPhos is coordinated to Ni (i.e., a κ^1-DiploPhos species).[5] Similar chemical shifts have been reported for the dissociated arm of a κ^1-dppb complex,[5] and we were able to observe κ^1-dppb species after performing the analogous experiments from (dppb)Ni(*o*-Tol)Cl (see Supporting Information Section S9.3.3). We attempted DOSY on **4** to determine its aggregation state in solution, but these attempts were unsuccessful.[52]

Motivated by our prior observations of diminished yields for substrates that do not possess Lewis basic functionality (**1e** and **1l**), we chose to investigate whether heteroarene additives could induce disaggregation from **4**. Upon mixing **4**, DiploPhos, and 50 equivalents of 4-trifluoromethylpyridine ($^{4\text{-CF}_3}$**py**) at ambient temperature (spectrum **C**), we saw the appearance of similar peaks to spectrum **B**, indicating that pyridines are able to break up tetrameric **4**. Despite the apparent interaction between **4** and $^{4\text{-CF}_3}$**py**, only unbound pyridine was observed by ^{19}F NMR at both 25 °C and –40 °C, consistent with a small population of pyridine-bound Ni species.[53]

To see how speciation of **4** influences reactivity in a catalytically relevant context, we performed kinetic studies on the stoichiometric transmetalation of tetrameric **4** with boronate **5** (Figure 6A).[5,6,31,54] Under these conditions, formation of the cross-coupled product **6** can be used to track the rate of transmetalation, as reductive elimination is assumed to be fast. Addition of 1 equivalent of DiploPhos (to give a DiploPhos/Ni ratio of 2:1) accelerated the transmetalation reaction, and addition of 1 equivalent of $^{4\text{-CF}_3}$**py** accelerated the reaction even further. Interestingly, the same additives led to a less pronounced acceleration for the analogous timecourses with dppb (see Supporting Information Section S9.4.2). We attribute the observed rate enhancement to Lewis base-induced disaggregation to generate more reactive κ^1-DiploPhos species (as observed in Figure 5E). These results also help explain the optimal 2:1 DiploPhos/Ni ratio in the catalytic reaction.

With the speciation studies and transmetalation timecourse data in hand, we were curious if our findings on the role of Lewis basic additives could lead to improvements in catalytic reactivity. We first evaluated the addition of 1 equivalent of $^{4\text{-CF}_3}$**py** for scope examples containing no Lewis bases (Figure 6B). Gratifyingly, we observed substantial increases in yield for both **1e** (from 28 to 39%) and **1l** (from 35 to 80%). In addition, we chose to evaluate the pyridine additive in a pair of couplings in which the identity of one partner was varied between an arene and a heteroarene. In the heteroaryl coupling—which affords product **1k**—the Ni/DiploPhos system gives similar yields regardless of the presence of pyridine (84 and 85% yield with and without $^{4\text{-CF}_3}$**py**, respectively). However, upon removal of the pyridine moiety in the substrate, cross-coupled product **7** is obtained in just 49% yield. Addition of 1 equivalent of $^{4\text{-CF}_3}$**py** to this Lewis-base free coupling restores reactivity to afford **7** in 79% yield.

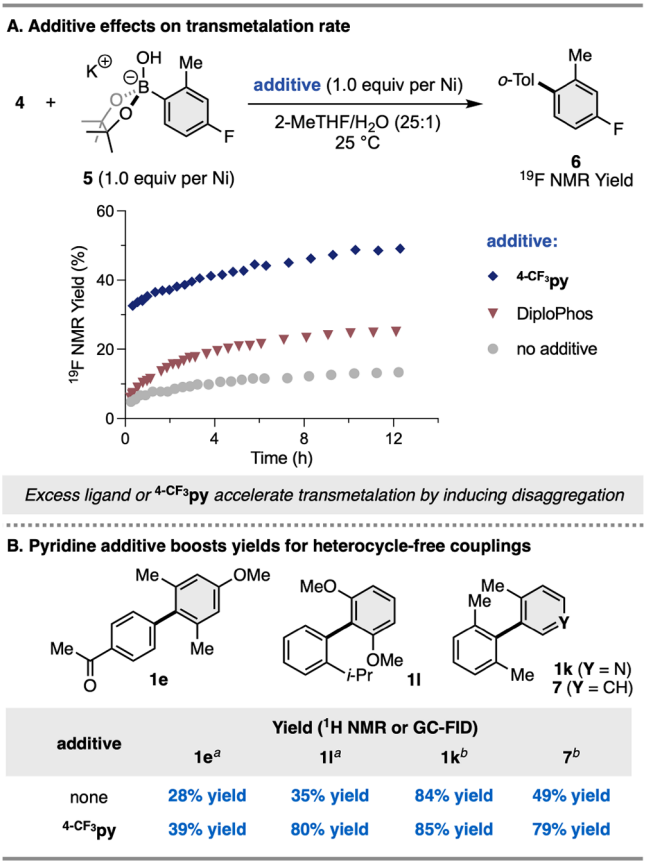

additive	Yield (^{1}H NMR or GC-FID)			
	1e[a]	**1l**[a]	**1k**[b]	**7**[b]
none	28% yield	35% yield	84% yield	49% yield
$^{4\text{-CF}_3}$**py**	39% yield	80% yield	85% yield	79% yield

Figure 6. (A) Timecourse tracking conversion of formation of 6 following the reaction between 4 and 5. The reaction's major byproduct is 3-fluorotoluene. Yields were determined by ^{19}F NMR using 2-fluorobiphenyl as an internal standard. (B) Effect of $^{4\text{-CF}_3}$**py** additive on the yield of cross-coupled products. Conditions: (TMEDA)Ni(*o*-Tol)Cl (2 mol %), DiploPhos (4.4 mol %), $^{4\text{-CF}_3}$**py** (0 or 1.0 equiv), K_3PO_4 (3.0 equiv), 2-MeTHF/H_2O = 2:1, 70 °C, 20 h. [a]Yields were determined by ^{1}H NMR using 1,3,5-trimethoxybenzene as an internal standard. [b]Yields were determined by GC-FID using 1,3,5-trimethoxybenzene as an internal standard.

With an improved understanding of the effect of heterocycles on speciation in the Ni/DiploPhos system, we returned to NMR studies to further characterize the behavior of κ^1-DiploPhos species formed following disaggregation. Notably, we observed line broadening in the free phosphine region in spectrum **B** (Figure 5E), implying ligand exchange between κ^1-DiploPhos and free DiploPhos. This observation prompted us to use variable-temperature (VT) NMR to investigate the kinetics of DiploPhos exchange among the species formed (Figure 7A). We conducted this experiment by mixing **4** and DiploPhos in 2-MeTHF and heating the NMR tube prior to acquiring spectra to induce formation of κ^1-DiploPhos species (vide supra). In parallel, we also evaluated the analogous exchange for dppb in order to better understand the effect of DiploPhos's remote steric bulk on speciation. For DiploPhos, no coalescence was observed up to 67 °C, which was the highest temperature evaluated due to solvent constraints. However, a lower bound on the exchange barrier ($\Delta G^{\ddagger}_{ex}$) could be

https://doi.org/10.1021/acscatal.6c05422
ACS Catal. XXXX, XXX, XXX–XXX

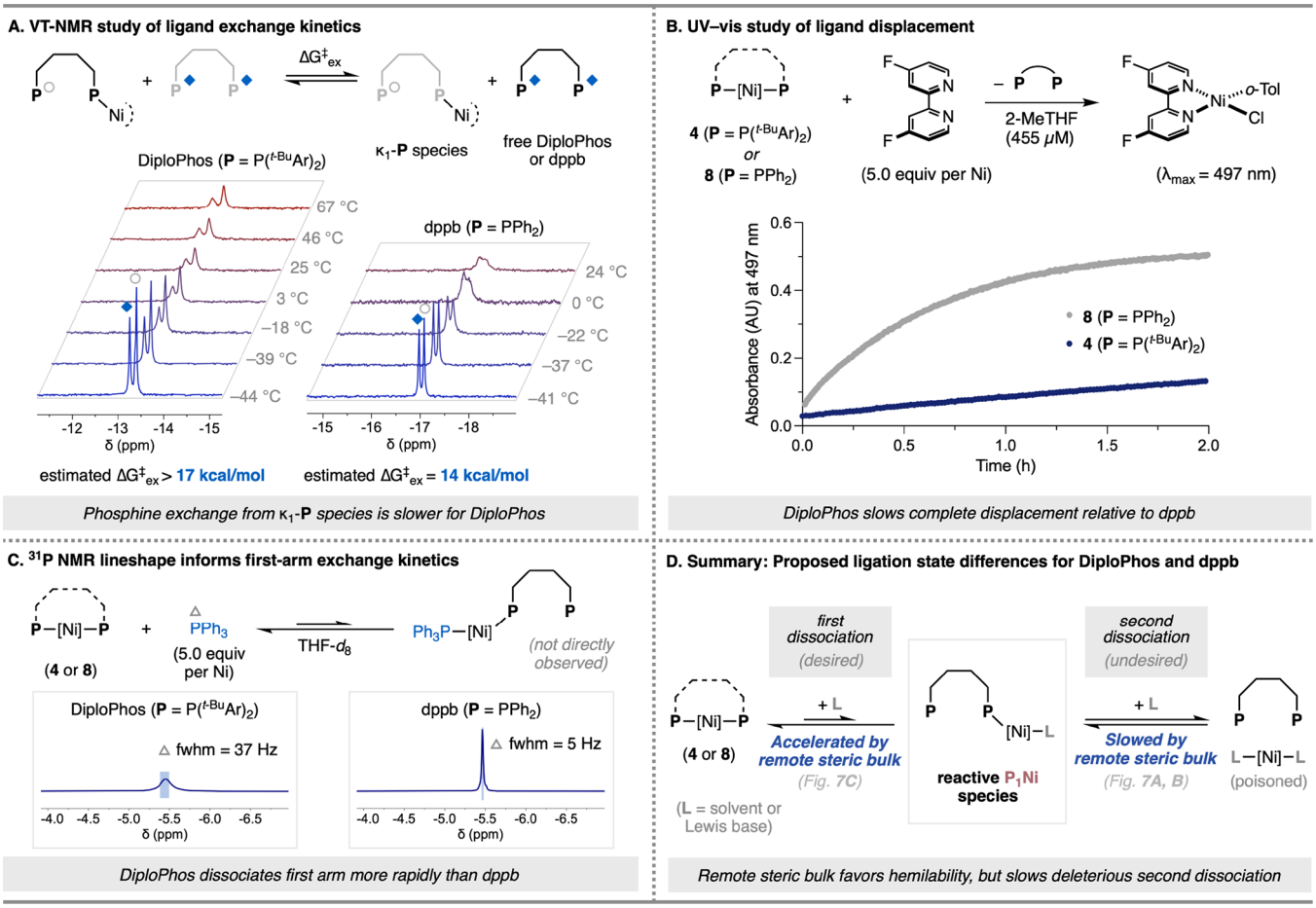

Figure 7. (A) Variable-temperature $^{31}P\{^{1}H\}$ NMR studies. Experiments were run with oxidative addition complex + 1.0 equivalent of bisphosphine per Ni in 2-MeTHF. (B) UV–vis timecourse of bisphosphine displacement with a bipyridine ligand. [Ni] = Ni(*o*-Tol)Cl (C) Line broadening of the PPh_3 resonance in ^{31}P NMR for solutions of OAC and 5 equiv PPh_3 (fwhm = full width at half maximum). (D) Summary of ligand dissociation kinetics.

estimated using an approximate solution to the Bloch equations (see Supporting Information Section S9.6.3).[55] Using the temperature of coalescence, as well as the peak separation in the slow-exchange regime at −44 °C, we estimate that $\Delta G^{\ddagger}_{ex} >$ 17 kcal/mol. For dppb, we observed the κ^1-dppb and free dppb resonances to merge at around 0 °C ($\Delta G^{\ddagger}_{ex} \sim$ 14 kcal/mol), implying slower exchange for DiploPhos than for dppb.

To corroborate this finding, we investigated the displacement of dppb or DiploPhos from their respective OACs (**4** or (dppb)Ni(*o*-Tol)Cl (**8**), Figure 7B). We chose to evaluate displacement by a bipyridine (bpy) ligand given their similarity to coordinating substrates and the characteristic UV–vis spectra of (bpy)Ni(*o*-Tol)Cl complexes.[56] 4,4′-Difluoro-2,2′-bipyridine (^{F}bpy) was chosen since it provided a ^{19}F NMR handle to track product formation. However, the reaction between OAC **8** and ^{F}bpy was too fast to follow at NMR concentrations, so we tracked the formation of (^{F}bpy)Ni(*o*-Tol)Cl at its λ_{max} (497 nm) with UV–vis under more dilute conditions. We found that dppb is displaced from OAC **8** much faster than DiploPhos from OAC **4.**

We interpret the UV–vis and VT-NMR results to describe the kinetics of the dissociation of the second phosphine arm of DiploPhos and dppb. However, we presumed that the lability of the first bisphosphine arm was more relevant to the improved reactivity of DiploPhos relative to dppb than the lability of the second arm. While we were unable to directly observe exchange between the free and bound arms on the NMR timescale with EXSY,[18] we were able to compare first-arm exchange kinetics using a 1D line-broadening study (Figure 7C).[57] We found that when the DiploPhos and dppb OACs were treated with PPh_3, the $^{31}P\{^{1}H\}$ NMR resonance of free PPh_3 underwent broadening. Displacement of both arms of DiploPhos or dppb by PPh_3 is thermodynamically disfavored, but we propose that the observed broadening corresponds to coordination of PPh_3 to a κ^1-bisphosphine complex. While no mixed-ligand complexes could be directly identified by $^{31}P\{^{1}H\}$ NMR, we observed greater than 7-fold line-broadening of the free PPh_3 resonance in the presence of the DiploPhos OAC **4** relative to dppb OAC **8.**

This observation suggests that exchange between free PPh_3 and this mixed-ligand species is more rapid for DiploPhos,[58] consistent with the first arm of DiploPhos being more labile than the first arm of dppb.

Taken together, these experiments support a model in which the remote steric bulk of DiploPhos accelerates dissociation of the first bisphosphine arm relative to dppb but disfavors dissociation of the second arm (Figure 7D). The first dissociation generates P_1Ni species, which have been implicated as active

https://doi.org/10.1021/acscatal.6c05422
ACS Catal. XXXX, XXX, XXX–XXX

intermediates during transmetalation and oxidative addition events.[18,31] The reluctance of DiploPhos's second arm toward dissociation could explain the Ni/DiploPhos system's unusual ability to prevent heterocycle poisoning and the formation of other off-cycle Ni species.

3. CONCLUSIONS

We combined our understanding of ligation state requirements in Ni-catalyzed SMCs with HTE-enabled ligand scaffold evaluation to design DiploPhos, a hemilabile bisphosphine ligand. DiploPhos enables the formation of unprecedented tetra- and tri-*ortho*-substituted bi-(hetero)aryl products via Ni catalysis. These challenging SMCs used 2 mol % of an air-stable Ni precatalyst and a scale-up-friendly homogeneous biphasic solvent system.

Mechanistic investigations revealed that DiploPhos is resistant to forming the thermodynamic sink $(bisphosphine)_2Ni$ at Ni(0). At Ni(II), the hemilability of DiploPhos allows for the formation of reactive P_1Ni species, but this hemilability also results in the formation of aggregates such as tetrameric $[(DiploPhos)Ni(o\text{-}Tol)Cl]_4$ (**4**). We found that aggregates could be broken up using coordinating additives such as excess ligand or Lewis basic nitrogen heterocycles. This finding led us to discover $^{4\text{-}CF_3}$**py** as a useful additive for boosting yields in heterocycle-free scope examples.

While the lability of the first phosphine arm imparts improved reactivity, we found through VT-NMR and UV–vis studies that DiploPhos's second arm is resistant to displacement. This observation accounts for DiploPhos's ability to keep Ni species on-cycle and resist heterocycle poisoning.

Flexible, bidentate phosphine ligands have seen limited use in Ni-catalyzed cross couplings, perhaps due to their promiscuity towards aggregate formation.[59] We anticipate that the observed structure–speciation relationships for DiploPhos and dppb will contribute to further developments in the design of hemilabile ligands, including efforts towards atroposelective Ni SMCs and other challenging cross-coupling reactions.[15]

4. METHODS

4.1. General Procedure for Ni/DiploPhos-Catalyzed Suzuki–Miyaura Coupling

Inside a nitrogen-filled glovebox, a 2× stock solution of nickel precatalyst was prepared by combining (TMEDA)Ni(*o*-Tol)Cl (3.6 mg, 0.012 mmol, 4 mol %), DiploPhos (23.1 mg, 0.0264 mmol, 8.8 mol %), and 2-MeTHF (200 μL) in a 4 mL vial equipped with a PTFE-coated stir bar. The mixture was stirred (720–900 rpm) at 70 °C for 1 h. The 2x stock solution was allowed to cool before use. To a separate 4 mL vial (reaction vial) equipped with a PTFE-coated stir bar, aryl bromide (0.3 mmol, 1.0 equiv), aryl boronic ester (0.33 mmol, 1.1 equiv), K_3PO_4 (191.0 mg, 0.9 mmol, 3.0 equiv), and 2-MeTHF (400 μL) were combined. 100 μL of the 2× Ni precatalyst solution was added to the reaction vial, followed by H_2O (250 μL). The vial was capped with a solid PTFE-lined vial cap and sealed with electrical tape. The reaction vial was stirred (720–900 rpm) at 70 °C for 20 h. After 20 h, the reaction was quenched by removing the vial cap and exposing the reaction to oxygen. The reaction mixture was diluted with EtOAc and water, and the mixture was extracted with EtOAc (3 × 5 mL). The combined organic layers were dried with anhydrous Na_2SO_4, filtered, and concentrated in vacuo. The crude mixture was purified by silica gel flash chromatography (EtOAc/hexane).

■ ASSOCIATED CONTENT

Supporting Information

The Supporting Information is available free of charge at https://pubs.acs.org/doi/10.1021/acscatal.6c05422.

Experimental procedures, experimental data, and characterization and spectral data for new compounds (PDF)

Accession Codes

Deposition Numbers 2504222 and 2505398 contain the supplementary crystallographic data for this paper. These data can be obtained free of charge via the joint Cambridge Crystallographic Data Centre (CCDC) and Fachinformationszentrum Karlsruhe Access Structures service.

■ AUTHOR INFORMATION

Corresponding Authors

Michael C. Haibach – *Process Chemistry, AbbVie Inc. North Chicago, Illinois 60064, United States;* orcid.org/0000-0001-8383-5633; Email: michael.haibach@abbvie.com

Abigail G. Doyle – *Department of Chemistry and Biochemistry, University of California Los Angeles, Los Angeles, California 90095, United States;* orcid.org/0000-0002-6641-0833; Email: abigaildoyle@g.ucla.edu

Authors

T. Judah Raab – *Department of Chemistry and Biochemistry, University of California Los Angeles, Los Angeles, California 90095, United States;* orcid.org/0000-0001-9449-5574

Hang Chi Ho – *Department of Chemistry and Biochemistry, University of California Los Angeles, Los Angeles, California 90095, United States*

Tyler Kerr – *Department of Chemistry and Biochemistry, University of California Los Angeles, Los Angeles, California 90095, United States;* orcid.org/0000-0002-0369-4883

Nari Tao – *Department of Chemistry and Biochemistry, University of California Los Angeles, Los Angeles, California 90095, United States*

Shashank Shekhar – *Process Chemistry, AbbVie Inc. North Chicago, Illinois 60064, United States;* orcid.org/0000-0002-1903-5380

Rafal Swiatowiec – *Process Chemistry, AbbVie Inc. North Chicago, Illinois 60064, United States*

Complete contact information is available at: https://pubs.acs.org/doi/10.1021/acscatal.6c05422

Author Contributions

[§]T.J.R. and H.C.H. contributed equally.

Notes

The authors declare no competing financial interest.

■ ACKNOWLEDGMENTS

Financial support was provided by NIGMS R35 GM126986 and the Camille and Henry Dreyfus Foundation ST-25-030. H.C.H. acknowledges the Croucher foundation for its scholarship for doctoral study. We thank Dr. Ta-Chung Ong and Hootan Roshandel for assistance with NMR experiments, and Duilio Cascio and Michael Sawaya for assistance with X-ray crystallography. We also thank Paris Dee for helpful discussions. These studies were supported by shared instrumentation grants

from the National Science Foundation under equipment grant CHE-1048804 and the NIH Office of Research Infrastructure Programs under grant S10OD028644. AbbVie contributed to the design, execution, and approval of this study. S.S, R.S, and M.C.H. are AbbVie employees and may own AbbVie stocks.

■ REFERENCES

(1) Martin, R.; Buchwald, S. L. Palladium-Catalyzed Suzuki–Miyaura Cross-Coupling Reactions Employing Dialkylbiaryl Phosphine Ligands. *Acc. Chem. Res.* **2008**, *41*, 1461–1473.
(2) Littke, A. F.; Fu, G. C. Palladium-Catalyzed Coupling Reactions of Aryl Chlorides. *Angew. Chem., Int. Ed.* **2002**, *41*, 4176–4211.
(3) Magano, J.; Dunetz, J. R. Large-Scale Applications of Transition Metal-Catalyzed Couplings for the Synthesis of Pharmaceuticals. *Chem. Rev.* **2011**, *111*, 2177–2250.
(4) Brown, D. G.; Boström, J. Analysis of Past and Present Synthetic Methodologies on Medicinal Chemistry: Where Have All the New Reactions Gone? *J. Med. Chem.* **2016**, *59*, 4443–4458.
(5) Guo, X.; Dang, H.; Wisniewski, S. R.; Simmons, E. M. Nickel-Catalyzed Suzuki–Miyaura Cross-Coupling Facilitated by a Weak Amine Base with Water as a Cosolvent. *Organometallics* **2022**, *41*, 1269–1274.
(6) Yang, J.; Neary, M. C.; Diao, T. ProPhos: A Ligand for Promoting Nickel-Catalyzed Suzuki-Miyaura Coupling Inspired by Mechanistic Insights into Transmetalation. *J. Am. Chem. Soc.* **2024**, *146*, 6360–6368.
(7) Yang, J.; Zhao, H.; Schultz, J. E.; Wisniewski, S. R.; Simmons, E. M.; Diao, T. Process-Ready Nickel-Catalyzed Suzuki–Miyaura Coupling Enabled by tri-ProPhos. *ACS Catal.* **2025**, *15*, 19302–19311.
(8) Islam, K.; Arora, V.; Vikas; Nag, B.; Kumar, A. Nickel Bromide Catalyzed Ligand-Free and Activator-less Suzuki Coupling Reactions. *ChemCatChem* **2022**, *14*, e202200440.
(9) Zim, D.; Monteiro, A. L. Suzuki Cross-Coupling of Aryl Halides with Aryl Boronic Acids Catalyzed by Phosphine-Free $NiCl_2{\cdot}6H_2O$. *Tetrahedron Lett.* **2002**, *43*, 4009–4011.
(10) Saeb, R.; Roh, B.; Cornella, J. "Naked Nickel"-Catalyzed Heteroaryl–Heteroaryl Suzuki–Miyaura Coupling. *Angew. Chem., Int. Ed.* **2025**, *64*, e202424051.
(11) Esteves, H. A.; Goldfogel, M. J.; Shemet, A.; Peng, C.; Hritzko, B.; Simmons, E. M.; Wisniewski, S. R. Advancing Base-Metal Catalysis: Developing Nickel Catalysis for the Direct Telescope of Miyaura Borylation and Suzuki–Miyaura Cross-Coupling Reactions. *Org. Process Res. Dev.* **2024**, *28*, 4039–4045.
(12) Dhital, R. N.; Sen, A.; Sato, T.; Hu, H.; Ishii, R.; Hashizume, D.; Takaya, H.; Uozumi, Y.; Yamada, Y. M. A. Activator-Promoted Aryl Halide-Dependent Chemoselective Buchwald–Hartwig and Suzuki–Miyaura Type Cross-Coupling Reactions. *Org. Lett.* **2020**, *22*, 4797–4801.
(13) Zhang, L.; Griffin, D. J.; Beaver, M. G.; Blue, L. E.; Borths, C. J.; Brown, D. B.; Caille, S.; Chen, Y.; Cherney, A. H.; Cochran, B. M.; Colyer, J. T.; Corbett, M. T.; Correll, T. L.; Crockett, R. D.; Dai, X.-J.; Dornan, P. K.; Farrell, R. P.; Hedley, S. J.; Hsieh, H.-W.; Huang, L.; Huggins, S.; Liu, M.; Lovette, M. A.; Quasdorf, K.; Powazinik, W.; Reifman, J.; Robinson, J. A.; Sangodkar, R. P.; Sharma, S.; Kumar, S. S.; Smith, A. G.; St-Pierre, G.; Tedrow, J. S.; Thiel, O. R.; Truong, J. V.; Walker, S. D.; Wei, C. S.; Wilsily, A.; Xie, Y.; Yang, N.; Parsons, A. T. Development of a Commercial Manufacturing Process for Sotorasib, a First-in-Class KRASG12C Inhibitor. *Org. Process Res. Dev.* **2022**, *26*, 3115–3125.
(14) Genov, M.; Almorín, A.; Espinet, P. Efficient Synthesis of Chiral 1,1′-Binaphthalenes by the Asymmetric Suzuki–Miyaura Reaction: Dramatic Synthetic Improvement by Simple Purification of Naphthylboronic Acids. *Chem. – Eur. J.* **2006**, *12*, 9346–9352.
(15) Xu, X.-Y.; Liu, L.-G.; Xu, L.-C.; Zhang, S.-Q.; Hong, X. Transfer Learning-Enabled Ligand Prediction for Ni-Catalyzed Atroposelective Suzuki–Miyaura Cross-Coupling Based on Mechanistic Similarity: Leveraging Pd Knowledge for Ni Discovery. *J. Am. Chem. Soc.* **2025**, *147*, 15318–15328.
(16) Tasker, S. Z.; Standley, E. A.; Jamison, T. F. Recent Advances in Homogeneous Nickel Catalysis. *Nature* **2014**, *509*, 299–309.
(17) Newman-Stonebraker, S. H.; Smith, S. R.; Borowski, J. E.; Peters, E.; Gensch, T.; Johnson, H. C.; Sigman, M. S.; Doyle, A. G. Univariate Classification of Phosphine Ligation State and Reactivity in Cross-Coupling Catalysis. *Science* **2021**, *374*, 301–308.
(18) Borowski, J. E.; Newman-Stonebraker, S. H.; Doyle, A. G. Comparison of Monophosphine and Bisphosphine Precatalysts for Ni-Catalyzed Suzuki–Miyaura Cross-Coupling: Understanding the Role of the Ligation State in Catalysis. *ACS Catal.* **2023**, *13*, 7966–7977.
(19) Ge, S.; Hartwig, J. F. Highly Reactive, Single-Component Nickel Catalyst Precursor for Suzuki–Miyuara Cross-Coupling of Heteroaryl Boronic Acids with Heteroaryl Halides. *Angew. Chem., Int. Ed.* **2012**, *51*, 12837–12841.
(20) Sylvester, K. T.; Wu, K.; Doyle, A. G. Mechanistic Investigation of the Nickel-Catalyzed Suzuki Reaction of N,O-Acetals: Evidence for Boronic Acid Assisted Oxidative Addition and an Iminium Activation Pathway. *J. Am. Chem. Soc.* **2012**, *134*, 16967–16970.
(21) Sawatzky, R.; Stradiotto, M. (DPEPhos)Ni(Mesityl)Br: An Air-Stable Pre-Catalyst for Challenging Suzuki–Miyaura Cross-Couplings Leading to Unsymmetrical Biheteroaryls. *Synlett* **2018**, *29*, 799–804.
(22) DiploPhos was named after the long-necked dinosaur Diplodocus due to its linker length.
(23) Hoshi, T.; Nakazawa, T.; Saitoh, I.; Mori, A.; Suzuki, T.; Sakai, J.; Hagiwara, H. Biphenylene-Substituted Ruthenocenylphosphine for Suzuki–Miyaura Coupling of Aryl Chlorides. *Org. Lett.* **2008**, *10*, 2063–2066.
(24) Ackermann, L.; Potukuchi, H. K.; Althammer, A.; Born, R.; Mayer, P. Tetra-Ortho-Substituted Biaryls through Palladium-Catalyzed Suzuki–Miyaura Couplings with a Diaminochlorophosphine Ligand. *Org. Lett.* **2010**, *12*, 1004–1007.
(25) Walker, S. D.; Barder, T. E.; Martinelli, J. R.; Buchwald, S. L. A Rationally Designed Universal Catalyst for Suzuki–Miyaura Coupling Processes. *Angew. Chem. Int. Ed.* **2004**, *116*, 1907–1912.
(26) Altenhoff, G.; Goddard, R.; Lehmann, C. W.; Glorius, F. An N-Heterocyclic Carbene Ligand with Flexible Steric Bulk Allows Suzuki Cross-Coupling of Sterically Hindered Aryl Chlorides at Room Temperature. *Angew. Chem., Int. Ed.* **2003**, *42*, 3690–3693.
(27) Hayes, H. L. D.; Wei, R.; Assante, M.; Geogheghan, K. J.; Jin, N.; Tomasi, S.; Noonan, G.; Leach, A. G.; Lloyd-Jones, G. C. Protodeboronation of (Hetero)Arylboronic Esters: Direct versus Prehydrolytic Pathways and Self-/Auto-Catalysis. *J. Am. Chem. Soc.* **2021**, *143*, 14814–14826.
(28) Cox, P. A.; Leach, A. G.; Campbell, A. D.; Lloyd-Jones, G. C. Protodeboronation of Heteroaromatic, Vinyl, and Cyclopropyl Boronic Acids: pH–Rate Profiles, Autocatalysis, and Disproportionation. *J. Am. Chem. Soc.* **2016**, *138*, 9145–9157.
(29) Li, C.; Sotorrios, L.; Boaler, P. J.; Olikauskas, V.; Amico, M.; García-Domínguez, A.; Leach, A. G.; Lloyd-Jones, G. C. The Boroxine–Boronic Acid Equilibrium. *J. Am. Chem. Soc.* **2025**, *147*, 38237–38253.
(30) Haibach, M. C.; Ickes, A. R.; Tcyrulnikov, S.; Shekhar, S.; Monfette, S.; Swiatowiec, R.; Kotecki, B. J.; Wang, J.; Wall, A. L.; Henry, R. F.; Hansen, E. C. Enabling Suzuki–Miyaura Coupling of Lewis-Basic Arylboronic Esters with a Nonprecious Metal Catalyst. *Chem. Sci.* **2022**, *13*, 12906–12912.
(31) Payard, P.-A.; Perego, L. A.; Ciofini, I.; Grimaud, L. Taming Nickel-Catalyzed Suzuki-Miyaura Coupling: A Mechanistic Focus on Boron-to-Nickel Transmetalation. *ACS Catal.* **2018**, *8*, 4812–4823.
(32) Yoshioka, S.; Wen, K.; Saito, S. Development of Effective Bidentate Diphosphine Ligands of Ruthenium Catalysts toward Practical Hydrogenation of Carboxylic Acids. *Bull. Chem. Soc. Jpn.* **2021**, *94*, 1510–1524.
(33) Shields, B. J.; Stevens, J.; Li, J.; Parasram, M.; Damani, F.; Alvarado, J. I. M.; Janey, J. M.; Adams, R. P.; Doyle, A. G. Bayesian

Reaction Optimization as a Tool for Chemical Synthesis. *Nature* **2021**, *590*, 89–96.
(34) Torres, J. A. G.; Lau, S. H.; Anchuri, P.; Stevens, J. M.; Tabora, J. E.; Li, J.; Borovika, A.; Adams, R. P.; Doyle, A. G. A Multi-Objective Active Learning Platform and Web App for Reaction Optimization. *J. Am. Chem. Soc.* **2022**, *144*, 19999–20007.
(35) Magano, J.; Monfette, S. Development of an Air-Stable, Broadly Applicable Nickel Source for Nickel-Catalyzed Cross-Coupling. *ACS Catal.* **2015**, *5*, 3120–3123.
(36) Shields, J. D.; Gray, E. E.; Doyle, A. G. A Modular, Air-Stable Nickel Precatalyst. *Org. Lett.* **2015**, *17*, 2166–2169.
(37) Yin, J.; Rainka, M. P.; Zhang, X.-X.; Buchwald, S. L. A Highly Active Suzuki Catalyst for the Synthesis of Sterically Hindered Biaryls: Novel Ligand Coordination. *J. Am. Chem. Soc.* **2002**, *124*, 1162–1163.
(38) Düfert, M. A.; Billingsley, K. L.; Buchwald, S. L. Suzuki-Miyaura Cross-Coupling of Unprotected, Nitrogen-Rich Heterocycles: Substrate Scope and Mechanistic Investigation. *J. Am. Chem. Soc.* **2013**, *135*, 12877–12885.
(39) Collins, K. D.; Glorius, F. A Robustness Screen for the Rapid Assessment of Chemical Reactions. *Nat. Chem.* **2013**, *5*, 597–601.
(40) Kim, S.; Goldfogel, M. J.; Gilbert, M. M.; Weix, D. J. Nickel-Catalyzed Cross-Electrophile Coupling of Aryl Chlorides with Primary Alkyl Chlorides. *J. Am. Chem. Soc.* **2020**, *142*, 9902–9907.
(41) Walther, D. Reaktionen von Heteroolefinen an Zentralmetallen in Niedrigen Oxidationsstufen: Stabile Aldehydkomplexe Des Nickel(O) Und Verwandte Verbindungen. *J. Organomet. Chem.* **1980**, *190*, 393–401.
(42) Greaves, M. E.; Ronson, T. O.; Lloyd-Jones, G. C.; Maseras, F.; Sproules, S.; Nelson, D. J. Unexpected Nickel Complex Speciation Unlocks Alternative Pathways for the Reactions of Alkyl Halides with Dppf-Nickel(0). *ACS Catal.* **2020**, *10*, 10717–10725.
(43) Clevenger, A. L.; Stolley, R. M.; Staudaher, N. D.; Al, N.; Rheingold, A. L.; Vanderlinden, R. T.; Louie, J. Comprehensive Study of the Reactions Between Chelating Phosphines and $Ni(Cod)_2$. *Organometallics* **2018**, *37*, 3259–3268.
(44) Jacot-Descombes; Lucas, T.; Kjell, J. *Morfeus*. https://github.com/digital-chemistry-laboratory/morfeus.
(45) Staudaher, N. D.; Stolley, R. M.; Louie, J. Synthesis, Mechanism of Formation, and Catalytic Activity of Xantphos Nickel π-Complexes. *Chem. Commun.* **2014**, *50*, 15577–15580.
(46) Yin, G.; Kalvet, I.; Englert, U.; Schoenebeck, F. Fundamental Studies and Development of Nickel-Catalyzed Trifluoromethylthiolation of Aryl Chlorides: Active Catalytic Species and Key Roles of Ligand and Traceless MeCN Additive Revealed. *J. Am. Chem. Soc.* **2015**, *137*, 4164–4172.
(47) Standley, E. A.; Smith, S. J.; Müller, P.; Jamison, T. F. A Broadly Applicable Strategy for Entry into Homogeneous Nickel(0) Catalysts from Air-Stable Nickel(II) Complexes. *Organometallics* **2014**, *33*, 2012–2018.
(48) Clark, J. S. K.; Ferguson, M. J.; McDonald, R.; Stradiotto, M. PAd2-DalPhos Enables the Nickel-Catalyzed C–N Cross-Coupling of Primary Heteroarylamines and (Hetero)Aryl Chlorides. *Angew. Chem., Int. Ed.* **2019**, *58*, 6391–6395.
(49) Clark, J. S. K.; Voth, C. N.; Ferguson, M. J.; Stradiotto, M. Evaluating 1,1′-Bis(Phosphino)Ferrocene Ancillary Ligand Variants in the Nickel-Catalyzed C–N Cross-Coupling of (Hetero)Aryl Chlorides. *Organometallics* **2017**, *36*, 679–686.
(50) Yang, L.; Powell, D. R.; Houser, R. P. Structural Variation in Copper(I) Complexes with Pyridylmethylamide Ligands : Structural Analysis with a New Four-Coordinate Geometry Index, τ_4. *Dalton Trans.* **2007**, *36*, 955–964.
(51) D'Accriscio, F.; Ohleier, A.; Nicolas, E.; Demange, M.; Boullay, O. T. D.; Saffon-Merceron, N.; Fustier-Boutignon, M.; Rezabal, E.; Frison, G.; Nebra, N.; Mézailles, N. [(Dcpp)Ni(η^2-Arene)] Precursors: Synthesis, Reactivity, and Catalytic Application to the Suzuki–Miyaura Reaction. *Organometallics* **2020**, *39*, 1688–1699.
(52) We also considered the possibility that **4** is monomeric in solution and forms a mixture of κ^1-DiploPhos species upon heating or addition of pyridines regardless of its initial aggregation state. However, we cannot distinguish this possibility from our hypotheses experimentally.
(53) While we could not observe pyridine-bound nickel species, we hypothesize that rapid ligand exchange with pyridine assists disaggregation, with an equilibrium that lies far towards the nickel-phosphine species. Typically, d^8 square planar complexes undergo associative substitution. However, the detailed mechanism of substitution in this case is outside the scope of our study.
(54) The mechanism of boron-to-nickel transmetalation is debated, and this experiment is not intended to distinguish between the commonly proposed pathways. For more discussions, see references 6 and 31.
(55) Huggins, M. T.; Kesharwani, T.; Buttrick, J.; Nicholson, C. Variable Temperature NMR Experiment Studying Restricted Bond Rotation. *J. Chem. Educ.* **2020**, *97*, 1425–1429.
(56) Cagan, D. A.; Bím, D.; Silva, B.; Kazmierczak, N. P.; McNicholas, B. J.; Hadt, R. G. Elucidating the Mechanism of Excited-State Bond Homolysis in Nickel–Bipyridine Photoredox Catalysts. *J. Am. Chem. Soc.* **2022**, *144*, 6516–6531.
(57) Bain, A. D. Chemical Exchange in NMR. *Prog. Nucl. Magn. Reson. Spectrosc.* **2003**, *43*, 63–103.
(58) Housecroft, C. E.; Fehlner, T. P. Main Group Chemistry on a Metal Framework. Reactions of $[(\mu\text{-H})Fe_3(CO)_9BH_2R]^-$ (R = H, CH_3) with Lewis Bases. *J. Am. Chem. Soc.* **1986**, *108*, 4867–4873.
(59) Clevenger, A. L.; Stolley, R. M.; Aderibigbe, J.; Louie, J. Trends in the Usage of Bidentate Phosphines as Ligands in Nickel Catalysis. *Chem. Rev.* **2020**, *120*, 6124–6196.